The mechanism of copper uptake by tyrosinase from Bacillus megaterium

Margarita Kanteev, Mor Goldfeder, Michał Chojnacki, Noam Adir & Ayelet Fishman

JBIC Journal of Biological Inorganic Chemistry

ISSN 0949-8257
Volume 18
Number 8

J Biol Inorg Chem (2013) 18:895-903
DOI 10.1007/s00775-013-1034-0

Springer

J Biol Inorg Chem (2013) 18:895–903
DOI 10.1007/s00775-013-1034-0

ORIGINAL PAPER

The mechanism of copper uptake by tyrosinase from *Bacillus megaterium*

Margarita Kanteev · Mor Goldfeder · Michał Chojnacki · Noam Adir · Ayelet Fishman

Received: 17 May 2013 / Accepted: 12 August 2013 / Published online: 6 September 2013

Abstract Tyrosinase belongs to the type 3 copper enzyme family, containing a dinuclear copper center, CuA and CuB. It is mainly responsible for melanin production in a wide range of organisms. Although copper ions are essential for the activity of tyrosinase, the mechanism of copper uptake is still unclear. We have recently determined the crystal structure of tyrosinase from *Bacillus megaterium* (TyrBm) and revealed that this enzyme has tighter binding of CuA in comparison with CuB. Investigating copper accumulation in TyrBm, we found that the presence of copper has a more significant effect on the diphenolase activity. By decreasing the concentration of copper, we increased the diphenolase to monophenolase activity ratio twofold. Using a rational design approach, we identified five variants having an impact on copper uptake. We have found that a major role of the highly conserved Asn205 residue is to stabilize the orientation of the His204 imidazole ring in the binding site, thereby promoting the correct coordination of CuB. Further investigation of these variants revealed that Phe197, Met61, and Met184, which are located at the entrance to the binding site, not only play a role in copper uptake, but are also important for enhancing the diphenolase activity. We propose a mechanism of copper accumulation by the enzyme as well as an approach to changing the selectivity of TyrBm towards L-dopa production.

Keywords Tyrosinase · Copper accumulation · *Bacillus megaterium* · Suicide inactivation

Abbreviations

BCA	Bicinchoninic acid
DSC	Differential scanning calorimetry
ICP-AES	Inductively coupled plasma atomic emission spectroscopy
PDB	Protein Data Bank
Tris	Tris(hydroxymethyl)aminomethane
TyrBm	Tyrosinase from *Bacillus megaterium*
TyrSc	Tyrosinase from *Streptomyces castaneoglobisporus*

Introduction

Copper is a vital element for life, required for numerous enzymes that participate in many metabolic processes [1]. Copper homeostasis in all organisms is tightly controlled as the presence of excess intracellular copper has been shown to produce free radicals which can damage lipids, proteins, and nucleic acids [2–4]. Conversely, copper deficiency in humans has been shown to be the cause of severe diseases [5]. Copper transport has been extensively investigated over the past few years, and several copper-specific transport systems have been identified and characterized. These include the CTR transmembrane permease [6], the ATX1

M. Kanteev and M. Goldfeder equally contributed to the article.

An interactive 3D complement page in Proteopedia is avaliable at http://proteopedia.org/w/Journal:JBIC:21.

Electronic supplementary material The online version of this article (doi:10.1007/s00775-013-1034-0) contains supplementary material, which is available to authorized users.

M. Kanteev · M. Goldfeder · M. Chojnacki · A. Fishman (✉)
Department of Biotechnology and Food Engineering,
Technion-Israel Institute of Technology, 32000 Haifa, Israel
e-mail: afishman@tx.technion.ac.il

N. Adir
Schulich Faculty of Chemistry,
Technion-Israel Institute of Technology, 32000 Haifa, Israel

metallochaperone family, and P-type ATPases. However, many questions pertaining to copper import, transfer, and regulation have not been fully answered [7]. One aspect of copper activity as a bound cofactor in proteins that clearly requires elucidation is how the ions arrive at their final active-site destination, in many cases found deeply embedded with the protein structure, whereas other cases include chaperones and copper transporters [8, 9].

Tyrosinase (EC 1.14.18.1) is a type 3 copper enzyme, and is ubiquitously distributed in all domains of life. Tyrosinase is mainly responsible for melanin formation, which leads to skin pigmentation or the browning of fruit and vegetables, but apparently has additional functions, for instance, as a component in wound healing and primary immune response [10, 11]. In the presence of molecular oxygen, tyrosinase catalyzes two sequential reactions; the hydroxylation of phenols to form *o*-diphenols (monophenolase activity) and the oxidation of *o*-diphenols to *o*-quinones (diphenolase activity) [10, 12]. The active site of tyrosinase is composed of six conserved histidine residues which coordinate two copper ions, denoted CuA and CuB [10, 13]. The type 3 copper family also includes catechol oxidases and hemocyanins, and all three protein families have very similar active-site structures. Catechol oxidases are strictly diphenolases, and hemocyanins act as an oxygen carrier in arthropods and mollusks [14, 15]. However, when an N-terminal fragment in hemocyanin from *Eurypelma californicum* was removed, the protein acquired low monophenolase and diphenolase activities [16]. This variation in activities indicates that the shells surrounding the active-site copper ions are critical for determination of substrate specificity and rate control [10, 17, 18].

Tyrosinase has great potential for the production of various *o*-diphenols (also referred to as substituted catechols). Catechols are important intermediates for the synthesis of pharmaceuticals, agrochemicals, flavors, polymerization inhibitors, and antioxidants [19–22]. However, the use of tyrosinases for catechol synthesis has been limited since their diphenolase activity is much greater than their monophenolase activity [23]. In addition, little is known about the contribution of copper to tyrosinase substrate specificity and its effect on the monophenolase-to-diphenolase activity ratio.

We recently determined the structure of a tyrosinase from the soil bacterium *Bacillus megaterium* (TyrBm) [24–26]. The structures of two other tyrosinases have been determined as well, each in the presence of an additional protein subunit. The mushroom *Agaricus bisporus* tyrosinase was crystallized in a complex with a lectin-like subunit, whose role is still unclear [27], whereas the structure of the tyrosinase from *Streptomyces castaneoglobisporus* (TyrSc) was determined in a complex with a caddie protein, which was suggested to act as a copper transporter for the enzyme [17]. On the basis of the latter, a molecular mechanism for copper transport from the caddie was recently proposed [9]. Although TyrBm shares 43 % homology with TyrSc, it does not require a caddie protein for activity, and thus an intriguing question arises: How does TyrBm acquire copper ions and transport them into the active site? We have previously observed that copper binding is variable in TyrBm [26]. Whereas CuA (at slightly fluctuating positions) was found in all crystal structures, CuB was found only in the structures obtained in the presence of excess copper. Therefore, we suggested that TyrBm has tighter binding of CuA than of CuB. To try to clarify the observed plasticity in copper binding by TyrBm, we have investigated copper accumulation by TyrBm. Using a rational design approach, we identified residues which participate in copper binding and contribute to the enzyme selectivity. By mapping these residues, we show that it is possible to better control this enzyme's activity, and propose a mechanism for copper accumulation in TyrBm.

Materials and methods

Expression, purification, and crystallization

TyrBm was isolated from soil samples, and the gene encoding the tyrosinase was cloned into *Escherichia coli* BL21 (DE3), expressed, purified, and crystallized as previously described [24–26].

Preparation of apo wild-type and mutant TyrBm

To obtain enzyme samples completely devoid of copper, protein samples were incubated with 50 mM EDTA and dialyzed against tris(hydroxymethyl)aminomethane (Tris)–HCl buffer (50 mM, pH 7.5) several times. Removal of copper was confirmed by inductively coupled plasma atomic emission spectroscopy (ICP-AES; see later).

Mutagenesis

Tyrosinase variants M61L, M184L, F197A, N205A, and N205D were created with a QuikChange® site-directed mutagenesis kit (Stratagene, La Jolla, CA, USA) as suggested by the manufacturer using the primers listed in Table S1. Verification of the mutations was obtained by sequencing. The purification steps were identical to those performed for the the wild type.

Activity assay on L-tyrosine and L-dopa

Tyrosinase monophenolase and diphenolase activity was determined by measuring the formation of L-dopachrome

from 1 mM L-tyrosine or L-dopa. The reaction was performed in 96-well plates for 8 min at 25 °C and monitored with a multiplate reader (OPTImax tunable microplate reader; Molecular Devices, Sunnyvale, CA, USA) at 475 nm. Each reaction well consisted of Tris–HCl buffer (50 mM, pH 7.5), $CuSO_4$ in a range of concentrations (0–100 μM), and apoenzyme at a concentration of 6 μg/ml (0.17 μM). The rate of dopachrome formation was defined as the slope of the linear zone of the absorbance versus time plot. All measurements were conducted in triplicate, and were repeated four times.

Inductively coupled plasma atomic emission spectroscopy

The copper content of TyrBm was measured using an inductively coupled plasma atomic emission spectrometer (iCap 6000 series, Thermo Scientific). $CuSO_4$ was added to the protein samples at a ratio of 2 mol of Cu^{2+} per mole of protein for incubation periods of 5 min, 30 min, and 6 h. Each sample was subsequently dialyzed three times against 4 l of Tris–HCl buffer (50 mM, pH 7.5) in order to remove non-specifically bound metal ions. The amount of bound Cu^{2+} was subsequently measured by ICP-AES.

Differential scanning calorimetry

Differential scanning calorimetry (DSC) measurements were conducted with a MicroCal VP-DSC differential scanning calorimeter. The reference cell contained a dialysis buffer and the reaction cell contained 1 ml of apoprotein (2 mg/ml) in Tris–HCl buffer (50 mM, pH 7.5); 1 mM $CuSO_4$ was added to the protein sample in order to check the effect of copper ions on protein stability. To obtain a baseline, buffer with $CuSO_4$ versus buffer without $CuSO_4$ was first run, and the resulting curve was subtracted from the sample curves. The measurements were performed by scanning from low to high temperature at 1 °C/min, and the data were processed with Origin.

Bicinchoninic acid based assay

The affinity of TyrBm towards copper was determined by the rate of copper uptake from the bicinchoninic acid (BCA)–copper complex. BCA is highly sensitive and specific for Cu(I), which rapidly forms an intense purple complex with BCA [28]. The reaction was performed in 96-well plates for 5 min at 25 °C and was monitored with a multiplate reader (OPTImax tunable microplate reader; Molecular Devices, Sunnyvale, CA, USA) at 355 nm. Each reaction well contained *N*-(2-hydroxyethyl)piperazine-*N*′-ethanesulfonic acid buffer (50 mM, pH 8), 0.07 % NaOH, 0.1 % (w/v) ascorbic acid, 0.004 % (w/v) BCA, and 15 μM $CuSO_4$. The reaction was initiated by the addition of 19 μg of the apoenzyme to the reaction well, and the decrease in absorption was measured. The rate of copper uptake was defined as the slope of the linear zone of the absorbance versus time plot. All measurements were conducted in triplicate, and were repeated four times.

Data collection and structure determination

X-ray diffraction data was collected at the European Synchrotron Radiation Facility (Grenoble, France), beamlines ID14-1 and ID23-1. All data were indexed, integrated, scaled, and merged using Mosflm and Scala [29]. The structures of TyrBm variants were solved by molecular replacement using Phaser [30] and the coordinates of wild-type TyrBm [Protein Data Bank (PDB) code 3NM8]. Refinement was performed using Phenix [31] and Refmac5 [32, 33], and manual model building, real-space refinement, and structure validation were performed using COOT [34]. Data collection, phasing, and refinement statistics are presented in Table 1.

PDB accession numbers

Coordinates and structure factors of TyrBm have been deposited in the RCSB PDB under accession codes 4J6T (for TyrBm variant F197A), 4J6U (for TyrBm variant N205A), and 4J6V (for TyrBm variant N205D).

Results and discussion

The influence of copper concentration on the activity of wild-type TyrBm

In our previous investigations, we used excess amounts of copper in our activity assays to allow for optimal enzymatic activity (60-fold molar excess, 10 μM CuSO4) [25, 26, 35, 36]. Here, we investigated the influence of copper concentration on the monophenolase and diphenolase activity of apo-TyrBm. Monophenolase activity was measured using L-tyrosine, whereas the diphenolase activity was assayed using L-dopa. Since both copper ions are required for enzymatic activity, the minimal copper concentration theoretically needed under our experimental conditions to obtain full occupancy of the active site (1:2 molar ratio of TyrBm to Cu) is 0.35 μM $CuSO_4$ for 0.17 μM protein. However, TyrBm activity at this concentration is negligible (Fig. 1a). Whereas the monophenolase activity increased significantly from 0 to 3.5 μM $CuSO_4$, and remained unaffected by higher concentrations of copper, the maximum diphenolase activity was reached

Table 1 Data collection and refinement statistics

	F197A (PDB code 4J6T)	N205A (PDB code 4J6U)	N205D (PDB code 4J6V)
X-ray data collection			
Space group	*P*21	*P*21	*P*21
Unit-cell parameters			
a (Å)	55.01	48.08	54.90
b (Å)	78.80	78.77	78.33
c (Å)	84.34	85.99	82.16
α (°)	90.00	90.00	90.00
β (°)	106.62	104.63	105.50
γ (°)	90	90	90
Resolution range	2.43–56.42	2.39–57.20	1.9–43.84
Observed reflections	81,669 (10,812)	83,328 (11,154)	180,152 (26,596)
Unique reflections	26,006 (3,732)	24,549 (3,526)	51,526 (7,531)
$I/\sigma(I)$[a]	7.3 (4.2)	6.4 (2.6)	11.7 (5.6)
R_{merge}[a,b]	0.104 (0.17)	0.099 (0.19)	0.069 (0.251)
Completeness[a]	99.4 (98.1)	98.9 (98.0)	97.6 (98.1)
Multiplicity[a]	3.1 (2.9)	3.4 (3.2)	3.5 (3.5)
Refinement			
$R(\%)/R_{free}(\%)$[c]	20.11/24.49	21.71/25.28	19.62/21.4
Amino acids	573	571	573
Total non-hydrogen atoms	4,903	4,800	5,036
Water molecules	209	123	341
Copper ions	4	0	2
Average *B* factor (Å), protein atoms	32.10	38.7	25.00
RMSD			
Bond length (Å)	0.009	0.016	0.014
Bond angle (°)	1.17	1.41	1.37
Ramachandran plot			
Favored regions (%)	96.13	95.59	96.30
Outliers (%)	0.18	0.35	0.35
Allowed (%)	3.69	4.06	3.35

PDB Protein Data Bank, *RMSD* root mean square deviation

[a] Values in *parentheses* are for the last shell

[b] $R_{merge} = \sum_{hkl}\sum_i |I_i(hkl) - \langle I(jkl)\rangle| / \sum_{hkl}\sum_i I_i(hkl)$, where I is the observed intensity, and $\langle I\rangle$ is the mean value of I

[c] $R/R_{free} = \sum_{hkl} ||F_{obs}| - |F_{calc}|| / \sum_{hkl} |F_{obs}|$, where R and R_{free} are calculated using the test reflections, respectively. The test reflections (5 %) were held aside and not used during the entire refinement process

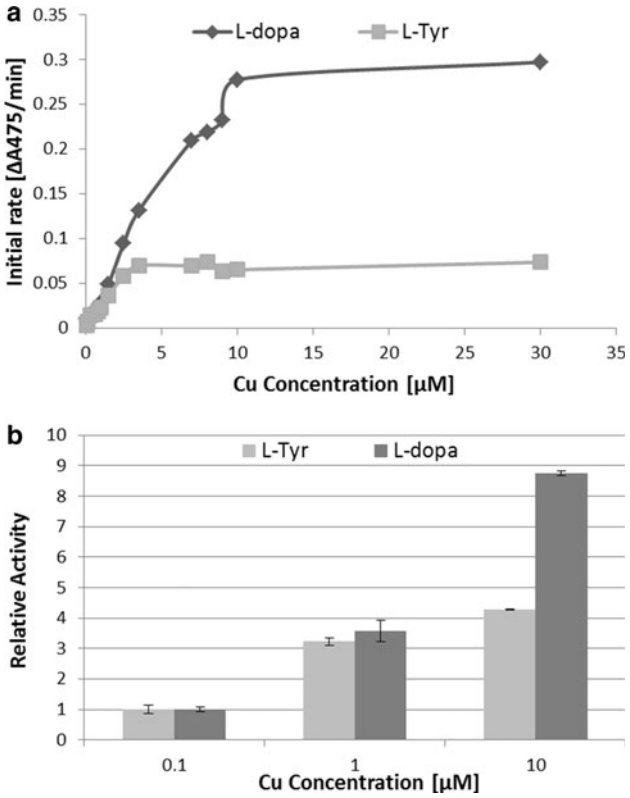

Fig. 1 Copper dependence of wild-type tyrosinase from *Bacillus megaterium* (TyrBm). **a** Activity on L-tyrosine and L-dopa at different concentrations of copper. **b** Relative activity on L-tyrosine and L-dopa in the presence of different copper concentrations (relative to the activity at 0.1 μM Cu). TyrBm activity was determined by monitoring the formation of L-dopachrome from 1 mM L-tyrosine or L-dopa at a wavelength of 475 nm. The rate of L-dopachrome formation was defined as the slope of the linear zone of the absorbance versus time plot and was plotted against the concentration of copper. All measurements were conducted in triplicate, and were repeated four times

only at 10 μM $CuSO_4$ (Fig. 1a). Copper concentrations higher than 30 μM inhibited both the monophenolase activity and the diphenolase activity (not shown). When the copper concentration was increased from 0.1 to 1 μM, the monophenolase and diphenolase activities increased by approximately 3.5-fold, and further increase in copper concentration affected mostly the diphenolase activity, which was improved by 8.5-fold, in contrast to the monophenolase activity, which was improved by fourfold (Fig. 1b). These results indicate that the diphenolase activity requires the presence of higher concentrations of copper than the monophenolase activity and the copper concentration appears to be a bottleneck of TyrBm's diphenolase activity. Two different research groups [37–40] propose that during the diphenolase activity, copper reduction occurs and a copper atom is released from the active site, which leads to suicide inactivation. Alternatively, it was shown by us that CuB is more loosely bound than CuA in TyrBm [26]. Therefore, it is possible that suicide inactivation occurs as a result of CuB ion release from the active site during the diphenolase activity. An attempt to quantify the release of copper following diphenolase activity using ICP-AES was unsuccessful

owing to the formation of colored melanin–copper aggregates [41].

Analysis of the TyrBm–Cu complex

The structural evidence showing the tight binding of CuA in TyrBm as opposed to the loss of CuB has raised questions regarding the mechanism of TyrBm binding copper, and regarding the enzyme's stability in the presence of copper. ICP-AES and DSC were used to analyze the TyrBm–Cu complex.

We determined the copper content of TyrBm by incubating apo-TyrBm samples with copper for different periods of time at a ratio of 2 mol of Cu^{2+} per mole of protein. This amount of copper is the minimal needed theoretically for full occupancy of the binding site (1:2 molar ratio of TyrBm to Cu), however it is less than the amount needed to obtain optimal activity (Fig. 1a). Unbound copper was removed by dialysis and bound copper was measured using ICP-AES. Our data demonstrate that incubation periods of 5 and 30 min were not sufficient to enable wild-type TyrBm to bind two copper ions. Only a prolonged incubation of 6 h resulted in full copper occupation (Table 2). These results indicate that under our experimental conditions, the rate of copper binding is slow when the amount of copper is limited.

The effect of copper ions on protein stability was analyzed using DSC. In this case the amount of copper added to the apoenzyme (1:16.5 molar ratio of TyrBm to Cu, equivalent to 3 μM $CuSO_4$ in the activity reaction) was higher than the amount used in the ICP-AES experiment. This copper concentration results in a significantly higher TyrBm activity (Fig. 1a). The results obtained by DSC showed that the presence of $CuSO_4$ substantially increased the thermal stability of wild-type TyrBm. The thermally induced unfolding of apo-TyrBm occurs as a single transition with T_m of 60 °C, but the addition of copper ions increased T_m of unfolding to 82 °C (Fig. 2). Similar results were reported for superoxide dismutases, where holoenzymes had significantly higher T_m than apoenzymes [42, 43]. The presence of copper in a sufficient amount therefore seems to stabilize the apoenzyme by binding to the active site.

Table 2 Copper content of wild-type tyrosinase from *Bacillus megaterium* (*TyrBm*) and variants as measured by inductively coupled plasma atomic emission spectroscopy

TyrBm variants[a]	Incubation period	Bound Cu atoms
Wild type	5 min	1.09 ± 0.25
	30 min	1.40 ± 0.10
	6 h	1.98 ± 0.13
N205D	6 h	1.42 ± 0.05
N205A	6 h	1.20 ± 0.08

[a] Average of three measurements

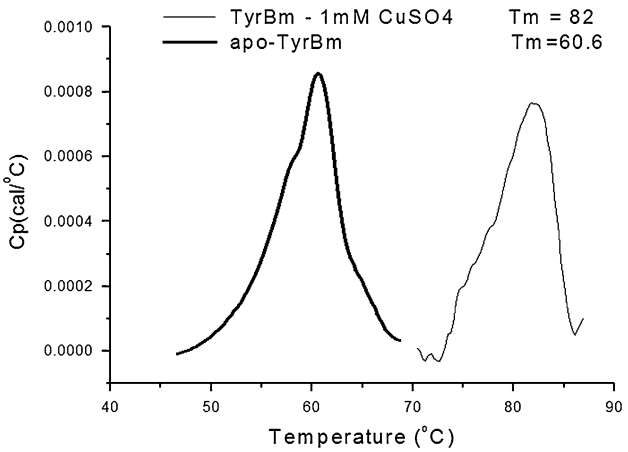

Fig. 2 Unfolding transitions of apo and metalated wild-type TyrBm. Differential scanning calorimetry scans at 1 °C/min demonstrating the effect of addition of copper on protein stability. Wild-type TyrBm (2 mg/ml) in tris(hydroxymethyl)aminomethane (Tris)–HCl buffer (50 mM, pH 7.5) with 1 mM $CuSO_4$ (*gray line*) or apo wild-type TyrBm (2 mg/ml) in Tris–HCl buffer (50 mM, pH 7.5) (*black line*)

Rational design for the investigation of copper binding

TyrBm variants M61L and M184L

Methionine residues are known to have the ability to ligate copper ions and are highly important for copper transport [44–50]. Analyzing the crystal structure of TyrBm [24, 26], we found that two adjacent methionine residues, Met61 and Met184, are located on the outer surface of the protein, at the entrance to the active site of TyrBm (Figs. 3a, S3). Similarly, in the structure of TyrSc in complex with the caddie protein (PDB code 1WX2), two methionine residues, spatially similar to the TyrBm Met61 and Met184, were revealed to be important for copper binding [9, 17]. To ascertain whether Met61 and Met184 have a role in copper transfer, we mutated these residues to leucine, which has a length and a volume similar to those of methionine. The relative affinity towards copper was tested by the ability of TyrBm variants M61L and M184L to take up copper from the BCA–Cu complex. Protein samples were added to the preformed BCA–Cu complex, and the change in absorption was monitored and compared with that of the wild type [28]. Similar experiments to determine the affinity and copper transfer between Atox1 and metal binding domains were performed by Yatsunyk and Rosenzweig [51]. Figure 5 shows that variants M61L and M184L have lower ability to compete with BCA for copper in comparison with the wild-type enzyme. Owing to the substitution of Met61 and Met184 with leucine, the ability to bind copper decreased by 30 and 40 %, respectively.

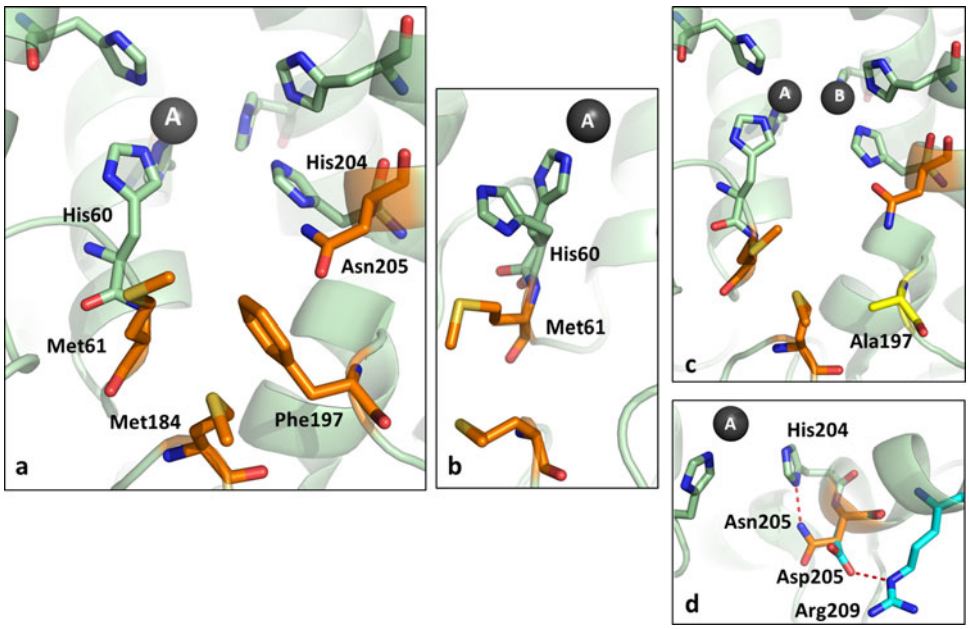

Fig. 3 Structure of wild-type TyrBm and variants. **a** The active site and the second-shell residues of wild-type TyrBm [Protein Data Bank (PDB) code 3NQ0]. Six histidine residues composing the active site are shown in a stick representation and in *pale green*. Residues Met61, Met184, Phe197, and Asn205 were investigated using site-directed mutagenesis and are shown in a stick representation in *orange*. CuA and CuB are shown as *gray spheres*. **b** The active site of variant V218F (PDB code 4HD4). Residues His60 and Met61 are shown in a stick representation in *pale green* and *orange*, respectively. Residue His60 is shown in two conformations, coordinating CuA in the active site or flipped out towards Met61. **c** The active site of variant F197A (PDB code 4J6T), with the alanine at this position in *yellow*. **d** Superposition of wild-type TyrBm (PDB code 3NQ0) and variant N205D (PDB code 4J6V). Histidine residues coordinating copper ions are in *pale green*, and Asn205 forming a hydrogen bond (*dashed red line*) with His204 is in *orange*. Asp205, in variant N205D, forms a hydrogen bond (*dashed red line*) with Arg209; both residues are shown in a stick representation in *cyan*

The monophenolase and diphenolase activities of variants M61L and M184L were measured with L-tyrosine and L-dopa in the presence of different copper concentrations, from 1 to 30 μM (Fig. 5). The monophenolase activity of both variants in the presence of 1–6 μM $CuSO_4$ increased gradually with the increase of copper concentration, but remained lower than the activity of the wild-type enzyme. Above 10 μM $CuSO_4$, the activity of variant M184L was similar to the activity of the wild type, whereas the activity of variant M61L was improved by approximately 1.5-fold. Poorer ability to take up copper and decreased monophenolase activity when copper is deficient suggest that Met61 and Met184 take part in binding and delivery of copper to the active site. Surprisingly, the diphenolase activity of these variants was significantly lower than the diphenolase activity in wild-type TyrBm, and this impairment could not be significantly overcome by increase of the copper concentration. As already mentioned, the diphenolase activity of TyrBm is more sensitive than the monophenolase activity to presence of copper (Fig. 1). Thus, if Met61 and Met184 are essential for copper binding, the effect on the diphenolase activity would indeed be more pronounced than the effect on the monophenolase activity. Moreover, it was recently reported that methionine residues, via their sulfur atom, form hydrophobic interactions with aromatic rings [52]. On the basis of these findings, it is possible that Met61 and Met184 are not only important for copper transfer, but also interact with the aromatic ring of substrates. As mentioned already, the substitution of Met61 with leucine improved the monophenolase activity of the enzyme when excess copper was present (Fig. 5a). Therefore, we suggest that in wild-type TyrBm, Met61 regulates the rate of the enzyme activity by participating in hydrophobic interactions with the aromatic ring of L-tyrosine. Furthermore, the results show that both methionine residues are essential for diphenolase activity. Possibly, by participating in hydrophobic interactions with the aromatic ring of L-dopa, these residues contribute to the "correct" orientation of the substrate in the binding site and decrease the effect of suicide inactivation [37, 38]. To support the suggested role of the methionine residues, we engineered two double mutation variants M61L/M184L and M61L/V218F (Fig. S2). Variant V218F was recently reported to significantly increase the monophenolase activity of TyrBm [35], and this was further shown over a wide range of copper concentrations (Fig. S2). At low copper concentrations, the monophenolase activity of both variants was low, but when copper was in excess, the monophenolase activity was higher in comparison with the monophenolase activity of the wild type. The diphenolase activity of both

variants was lower than that of the wild type [35]. This result strengthens our suggestion that Met61 and Met184 are vital for TyrBm activity at low copper concentrations. Furthermore, in both double mutants the substitution of Met61with leucine improves the monophenolase activity at higher copper concentrations.

TyrBm variants N205A and N205D

Asn205 is also located in the active-site entrance of TyrBm (Figs. 3a, S3) and was previously reported to interact with the tyrosinase inhibitor kojic acid [11, 26]. Although Asn205 is highly conserved among tyrosinases, its role is still unclear [53]. Substitution of either alanine or aspartic acid for Asn205 induced a significant reduction in the activities on both substrates (Fig. 5) and in the rate of copper uptake (Fig. 4). ICP-AES analysis showed that even after incubation with $CuSO_4$ for 6 h, the copper contents in variants N205A and N205D were 1.2 and 1.4 mol of copper per mole of protein, respectively (Table 2). Therefore, we suggest that the mutation at position 205 in TyrBm affects copper occupancy. In the crystal structure of wild-type TyrBm [24, 26], Asn205 forms a polar bond with the imidazole ring of His204, which coordinates CuB in the active site (Fig. 3d). We determined the crystal structures of variants N205A and N205D (Table 2), and found the overall structures of these variants were similar to the structure of the wild type [24]. However, Asp205 in the structure of variant N205D is turned towards Arg209 and therefore cannot form a polar bond with His204 (Figs. 3d, S1b). It seems that one of the roles of Asn205 is to stabilize His204 in an orientation that provides the most efficient coordination of CuB in the active site.

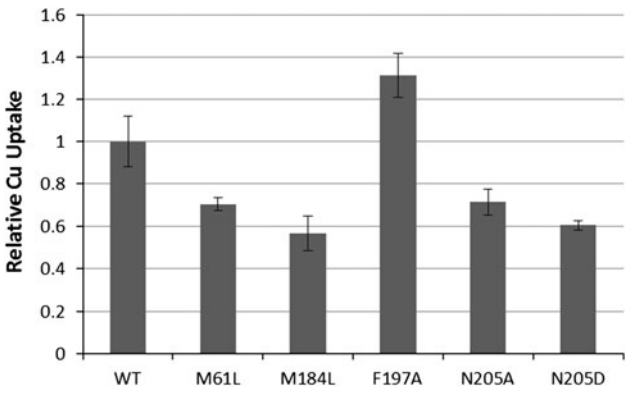

Fig. 4 Relative copper uptake of TyrBm variants. The relative copper uptake of TyrBm variants towards copper was determined by the ability of the enzyme to take up copper from a bicinchoninic acid (BCA)–Cu complex in comparison with the ability of the wild-type enzyme. Copper uptake was determined by monitoring the disappearance of the absorbance of the BCA–Cu complex at 355 nm. *WT* wild type

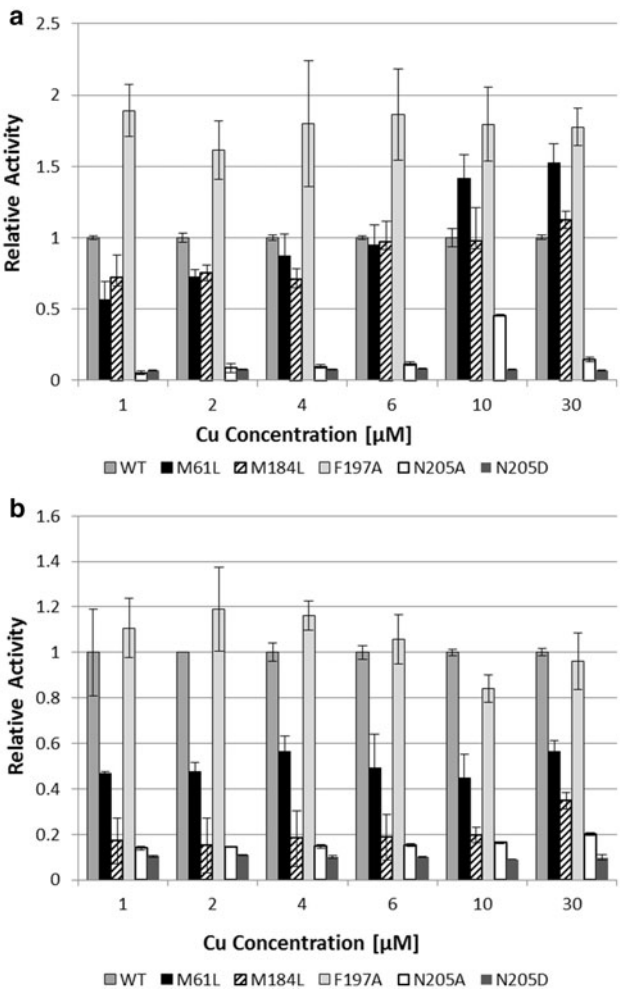

Fig. 5 Relative monophenolase to diphenolase activity ratio of TyrBm variants. **a** Monophenolase activity of TyrBm variants was measured with 1 mM L-tyrosine. **b** Diphenolase activity was measured with 1 mM L-dopa. The activity of TyrBm variants was measured in the presence of six different copper concentrations and was compared with the activity of the wild type. The activities were determined by monitoring the formation of L-dopachrome at 475 nm. All measurements were conducted in triplicate, and were repeated four times. *WT* wild type

TyrBm variant F197A

Phe197 is also located in the active-site entrance of TyrBm and was also observed to interact with kojic acid [26]. This residue was mutated to alanine and investigated in comparison with the wild type. Although the alanine residue at position 197 had little effect on the diphenolase activity of variant F197A (Fig. 5b), the rate of copper uptake was increased and the monophenolase activity was improved by approximately twofold (Figs. 4, 5a). Several crystal structures of variant F197A were determined at high resolution, and one of them is presented here (Table 2, Figs. 3c, S1a). In contrast to the structures of wild-type TyrBm, which usually contain only CuA [24, 25], all the structures of

variant F197A contained both copper ions. Apparently, the bulky Phe197 reduces the rate of uptake of CuB into the active site, whereas the substitution with a small alanine residue increased the rate of copper uptake and thus the rate of enzymatic activity (Figs. 4, 5). It seems that one of the roles of Phe197 might be to regulate copper uptake in TyrBm, perhaps in the absence of a substrate.

Improving the monophenolase to diphenolase activity ratio

We recently reported that TyrBm variants R209H and V218F improve the monophenolase to diphenolase activity ratio [35, 36, 54]. In the present study, we used a rational design approach to find residues in TyrBm which may play a role in incorporation of copper into the binding site, but may also affect the activity ratio. Although variant M61L inhibited copper uptake and F197A increased it, both variants improved the activity of TyrBm towards L-tyrosine. Variant M61L exhibited a monophenolase to diphenolase activity ratio threefold higher than that of the wild-type, whereas F197A had a twofold higher ratio. We propose that in both cases, the altered activity was a result of impairment of the hydrophobic interactions that typically occurs between the wild-type enzyme and the substrates. As mentioned already, replacing Met61 with leucine prevents the hydrophobic interactions between the methionine residue and the aromatic ring of the substrates [52]. Similarly, alanine cannot assist in correct orientation of the substrates entering the active site in variant F197A. It seems that in both variants the substrates have easier access to the active site. In the case of tyrosine, this results in higher activity, but in the case of L-dopa, this promotes suicide inactivation as a result of imperfect orientation and stabilization. We propose that the stabilization of L-dopa is essential for decreasing the effect of the suicide inhibition, whereas the activity on L-tyrosine is affected only by the accessibility to the active site.

In addition, we found that in the presence of 1–2 μM $CuSO_4$, wild-type TyrBm exhibited a monophenolase to diphenolase activity ratio 1.8-fold higher than in the presence of 10 μM $CuSO_4$. Therefore, we suggest that in order to alter the selectivity of TyrBm towards L-dopa production, the copper concentration should be decreased, and the accessibility of L-tyrosine to the active site should be increased.

Proposed pathway for copper accumulation

On the basis of our biochemical measurements and structural observations, we propose a pathway of copper accumulation. There are a number of indications that CuA and CuB enter the active site of TyrBm by two different pathways. In all structures of TyrBm (besides that of variant F197A), only CuA was fully observed in the active site. Also, the second-shell residues around CuB are highly conserved in contrast to CuA binding site residues [53]. One of the coordinating residues of CuA in the active site is His60 (Figs. 3a, S3). This residue was previously observed to be stabilized in two alternative conformations, and this flexibility of His60 was attributed to promoting enzymatic activity [17, 35]. According to our recently determined crystal structure (PDB code 4HD4) [35], the flipped-out conformation of His60 turns towards Met61 (Fig. 3b). In the present study, we have shown that Met61 and Met184 take part in copper uptake. Therefore, we suggest that a copper ion entering the active site (CuA) first associates with the methionine residues, followed by its transfer to His60 in its flipped-out conformation (Fig. 3b). Following copper binding, His60 alters its conformation and transfers CuA to the active site in a paddle-like motion. Since the replacement of methionine residues did not have a drastic effect on copper uptake or on TyrBm activity (Figs. 4, 5), we believe that the role of Met61 and Met184 is to facilitate copper uptake when copper availability is minimal.

We propose that CuB passes only through Asp205 and Phe197 (Figs. 3a, S3). We have demonstrated here that the substitution of residues Asp205 and Phe197 affected both copper uptake and activity (Figs. 4, 5). Moreover, the proposed pathway clarifies the previously reported observations of TyrBm's tighter binding of CuA in comparison with CuB [17].

Acknowledgments This work was supported by the Israel Science Foundation founded by the Israel Academy of Sciences and Humanities, grant number 193/11. We gratefully thank the staff of the European Synchrotron Radiation Facility (beamlines ID23-1 and ID14-4) for provision of synchrotron radiation facilities and assistance.

References

1. Gadd GM (1992) FEMS Microbiol Lett 100:197–203
2. Peña MMO, Koch KA, Thiele DJ (1998) Mol Cell Biol 18:2514–2523
3. Aust SD, Morehouse LA, Thomas CE (1985) J Free Radic Biol Med 1:3–25
4. Rolff M, Schottenheim J, Decker H, Tuczek F (2011) Chem Soc Rev 40:4077–4098
5. Waggoner DJ, Bartnikas TB, Gitlin JD (1999) Neurobiol Dis 6:221–230
6. Dancis A, Yuan DS, Haile D, Askwith C, Eide D, Moehle C, Kaplan J, Klausner RD (1994) Cell 76:393–402
7. Huffman DL, O'Halloran TV (2001) Annu Rev Biochem 70:677–701
8. Rae TD, Schmidt PJ, Pufahl RA, Culotta VC, O'Halloran TV (1999) Science 284:805–808
9. Matoba Y, Bando N, Oda K, Noda M, Higashikawa F, Kumagai T, Sugiyama M (2011) J Biol Chem 286:30219–30231
10. Claus H, Decker H (2006) Syst Appl Microbiol 29:3–14

11. Chang T-S (2009) Int J Mol Sci 10:2440–2475
12. Burton SG (2003) Trends Biotechnol 21:543–549
13. Decker H, Schweikardt T, Nillius D, Salzbrunn U, Jaenicke E, Tuczek F (2007) Gene 398:183–191
14. van Holde KE, Miller KI, Decker H (2001) J Biol Chem 276:15563–15566
15. Itoh S, Fukuzumi S (2007) Acc Chem Res 40:592–600
16. Decker H, Rimke T (1998) J Biol Chem 273:25889–25892
17. Matoba Y, Kumagai T, Yamamoto A, Yoshitsu H, Sugiyama M (2006) J Biol Chem 281:8981–8990
18. Wood JM, Decker H, Hartmann H, Chavan B, Rokos H, Spencer JD, Hasse S, Thornton MJ, Shalbaf M, Paus R, Schallreuter KU (2009) FASEB J 23:2065–2075
19. Halaouli S, Asther M, Sigoillot J, Hamdi M, Lomascolo A (2006) J Appl Microbiol 100:219–232
20. Kawamura-Konishi Y, Tsuji M, Hatana S, Asanuma M, Kakuta D, Kawano T, Mukouyama E, Goto H, Suzuki H (2007) Biosci Biotechnol Biochem 71:1752–1760
21. Nolan L, O'Connor K (2007) Biotechnol Lett 29:1045–1050
22. Wang G, Aazaz A, Peng Z, Shen P (2000) FEMS Microbiol Lett 185:23–27
23. Hernandez-Romero D, Sanchez-Amat A, Solano F (2006) FEBS J 273:257–270
24. Sendovski M, Kanteev M, Shuster V, Adir N, Fishman A (2010) Acta Crystallogr Sect F Struct Biol Cryst Commun 66:1101–1103
25. Shuster V, Fishman A (2009) J Mol Microbiol Biotechnol 17:188–200
26. Sendovski M, Kanteev M, Shuster Ben-Yosef V, Adir N, Fishman A (2011) J Mol Biol 405:227–237
27. Ismaya WT, Rozeboom HJ, Weijn A, Mes JJ, Fusetti F, Wichers HJ, Dijkstra BW (2011) Biochemistry 50:5477–5486
28. Brenner AJ, Harris ED (1995) Anal Biochem 226:80–84
29. Leslie AGW (1992) In: Wolf WM, Wilson KS (eds) Joint CCP4 + ESF-EAMCB newsletter on protein crystallography 26. Science and Engineering Research Council, Daresbury, and EMBL, Hamburg
30. McCoy AJ (2007) Acta Crystallogr Sect D Biol Crystallogr 63:32–41
31. Adams PD, Afonine PV, Bunkoczi G, Chen VB, Davis IW, Echols N, Headd JJ, Hung LW, Kapral GJ, Grosse-Kunstleve RW, McCoy AJ, Moriarty NW, Oeffner R, Read RJ, Richardson DC, Richardson JS, Terwilliger TC, Zwart PH (2010) Acta Crystallogr D Biol Crystallogr 66:213–221
32. Murshudov GN, Vagin AA, Dodson EJ (1997) Acta Crystallogr Sect D Biol Crystallogr 53:240–255
33. Skubak P, Murshudov GN, Pannu NS (2004) Acta Crystallogr Sect F Struct Biol Cryst Commun 60:2196–2201
34. Emsley P, Cowtan K (2004) Acta Crystallogr Sect D Biol Crystallogr 60:2126–2132
35. Goldfeder M, Kanteev M, Adir N, Fishman A (2013) Biochim Biophys Acta 1834:629–633
36. Goldfeder M, Egozy M, Shuster Ben-Yosef V, Adir N, Fishman A (2012) Appl Microbiol Biotechnol 97:1953–1961
37. Muñoz-Muñoz JL, Garcia-Molina F, Varon R, Garcia-Ruíz PA, Tudela J, Garcia-Cánovas F, Rodríguez-López JN (2010) IUBMB Life 62:539–547
38. Ramsden C, Riley P (2010) ARKIVOC (i):260–274
39. Muñoz-muñoz JL, García-molina F, García-ruiz PA, Molina-alarcón M, Tudela J, García-cánovas F, Rodríguez-lópez JN (2008) Biochem J 416:431–440
40. Ramsden CA, Stratford MR, Riley PA (2009) Org Biomol Chem 7:3388–3390
41. Gallas J, Littrell K, Seifert S, Zajac G, Thiyagarajan P (1999) Biophys J 77:1135–1142
42. Mizuno K, Whittaker MM, Bachinger HP, Whittaker JW (2004) J Biol Chem 279:27339–27344
43. Dolashka-Angelova P, Angelova M, Genova L, Stoeva S, Voelter W (1999) Spectrochim Acta Part A Mol Biomol Spectrosc 11:2249–2260
44. Bauman AT, Broers BA, Kline CD, Blackburn NJ (2011) Biochemistry 50:10819–10828
45. Larson CA, Adams PL, Blair BG, Safaei R, Howell SB (2010) Mol Pharmacol 78:333–339
46. Shimizu A, Sasaki T, Kwon JH, Odaka A, Satoh T, Sakurai N, Sakurai T, Yamaguchi S, Samejima T (1999) J Biochem 125:662–668
47. Chang T, Iverson S, Rodrigues C, Kiser C, Lew A, Germanas J, Richards J (1991) Proc Natl Acad Sci USA 88:1325–1329
48. Gourdon P, Liu XY, Skjorringe T, Morth JP, Moller LB, Pedersen BP, Nissen P (2011) Nature 475:59–64
49. Guo Y, Smith K, Lee J, Thiele DJ, Petris MJ (2004) J Biol Chem 279:17428–17433
50. Singh SK, Roberts SA, McDevitt SF, Weichsel A, Wildner GF, Grass GB, Rensing C, Montfort WR (2011) J Biol Chem 286:37849–37857
51. Yatsunyk LA, Rosenzweig AC (2007) J Biol Chem 282:8622–8631
52. Valley CC, Cembran A, Perlmutter JD, Lewis AK, Labello NP, Gao J, Sachs JN (2012) J Biol Chem 287:34979–34991
53. Schweikardt T, Olivares C, Solano F, Jaenicke E, Garcia-Borron JC, Decker H (2007) Pigm Cell Res 20:394–401
54. Shuster Ben-Yosef V, Sendovski M, Fishman A (2010) Enzyme Microb Technol 47:372–376